THE JOURNAL OF BIOLOGICAL CHEMISTRY VOL. 287, NO. 14, pp. 11325–11337, March 30, 2012

Insights into Hemoglobin Assembly through *in Vivo* Mutagenesis of α-Hemoglobin Stabilizing Protein*[S]

Received for publication, October 12, 2011, and in revised form, January 7, 2012 Published, JBC Papers in Press, January 27, 2012, DOI 10.1074/jbc.M111.313205

Eugene Khandros[‡], Todd L. Mollan[§1], Xiang Yu[‡], Xiaomei Wang[¶], Yu Yao[¶], Janine D'Souza[¶], David A. Gell[‖], John S. Olson[§], and Mitchell J. Weiss[‡¶2]

From the [‡]Cell and Molecular Biology Graduate Group, University of Pennsylvania, Philadelphia, Pennsylvania 19104, [§]Biochemistry and Cell Biology Department, Rice University, Houston, Texas 77251, [‖]Menzies Research Institute, University of Tasmania, Hobart, Tasmania 7000, Australia, and [¶]Division of Hematology, The Children's Hospital of Philadelphia, Philadelphia, Pennsylvania 19104

Background: The α-hemoglobin-stabilizing protein (AHSP) facilitates hemoglobin assembly.
Results: AHSP mutations that enhance binding affinity for α-globin or slow its rate of autooxidation *in vitro* do not affect normal or stressed erythropoiesis in mice.
Conclusion: AHSP exhibits robust molecular chaperone activity *in vivo* even when its biochemical interactions with reduced α-globin are perturbed.
Significance: Our findings support new models for AHSP activities *in vivo*.

α-Hemoglobin stabilizing protein (AHSP) is believed to facilitate adult Hemoglobin A assembly and protect against toxic free α-globin subunits. Recombinant AHSP binds multiple forms of free α-globin to stabilize their structures and inhibit precipitation. However, AHSP also stimulates autooxidation of αO_2 subunit and its rapid conversion to a partially unfolded bishistidyl hemichrome structure. To investigate these biochemical properties, we altered the evolutionarily conserved AHSP proline 30 in recombinantly expressed proteins and introduced identical mutations into the endogenous murine *Ahsp* gene. *In vitro*, the P30W AHSP variant bound oxygenated α chains with 30-fold increased affinity. Both P30W and P30A mutant proteins also caused decreased rates of αO_2 autooxidation as compared with wild-type AHSP. Despite these abnormalities, mice harboring P30A or P30W *Ahsp* mutations exhibited no detectable defects in erythropoiesis at steady state or during induced stresses. Further biochemical studies revealed that the AHSP P30A and P30W substitutions had minimal effects on AHSP interactions with ferric α subunits. Together, our findings indicate that the ability of AHSP to stabilize nascent α chain folding intermediates prior to hemin reduction and incorporation into adult Hemoglobin A is physiologically more important than AHSP interactions with ferrous αO_2 subunits.

Adult Hemoglobin A (HbA)[3] production *in vivo* is a highly coordinated process requiring balanced synthesis of individual α- and β-globin chains and their assembly with ferroprotoporphyrin IX (heme) prosthetic groups to form $\alpha_2\beta_2$ tetramers (1–3). Fully assembled HbA is very stable in comparison with isolated α and β subunits in their heme (Fe^{2+})- or hemin (Fe^{3+})-containing (holo) and heme-lacking (apo) forms (4, 5). Free α subunits, especially the Fe^{3+} (ferric) form, tend to catalyze the production of reactive oxygen species (ROS), denature, and form damaging precipitates (4, 6, 7).

Erythroid cells contain protective mechanisms to balance HbA synthesis and reduce the toxicity of free globin chains (8). For example, α-hemoglobin stabilizing protein (AHSP) binds α but not β chains or intact HbA (9, 10) and inhibits denaturation of free α-globin *in vitro* (9, 10). Targeted deletion of the *Ahsp* gene in mice causes globin precipitation, mild hemolytic anemia, and enhanced sensitivity to oxidant stress (10, 11). Loss of AHSP also aggravates both β-thalassemia (11) and α-thalassemia (12) in mice. In humans, several naturally occurring α-globin missense mutations and AHSP variants appear to cause anemia by inhibiting the ability of α-globin to interact with AHSP (13–17).

Recent studies have helped to define the biochemical and structural features of AHSP/α interactions (15, 18–23). AHSP is comprised of three antiparallel α helices with 11 unstructured amino acids at the carboxyl terminus (21–23). AHSP helix 1, helix 2, and the interconnecting loop interact with helices G and H of α-globin at a surface that overlaps with the interface for β-globin binding. However, β subunits bind α sub-

* This work was supported, in whole or in part, by National Institutes of Health Grants DK061692 (to M. J. W.), HL087427 (to M. J. W.), HL47020 (to J. S. O.), GM35649 (to J. S. O.), GM008362 (to T. L. M. through the Biotechnology Predoctoral Training Program at Rice University), and 3T32GM007170-35S1 (to E. K. through the NHLBI Medical Scientist Training Program). This work was also supported by Robert A. Welch Foundation Grant C-0612 (to J. S. O.) and the DiGaetano family.
[S] This article contains supplemental Figs. 1–3 and Tables 1–3.
[1] A Robert A. Welch Foundation predoctoral fellow.
[2] To whom correspondence should be addressed: Division of Hematology, The Children's Hospital of Philadelphia, The Abramson Research Center 316B, 3615 Civic Center Blvd., Philadelphia, PA 19104-4318. Tel.: 215-590-0565; Fax: 267-426-5476; E-mail: weissmi@email.chop.edu.

[3] The abbreviations used are: HbA, adult Hemoglobin A; apo, heme-lacking; bishistidyl conformation, ferric heme iron hexacoordinated with the proximal (E7) and distal (F8) histidines bound axially; DCFH, 2′,7′-dichlorofluorescein diacetate; ferric, Fe^{3+}; ferrous, Fe^{2+}; Hb, hemoglobin; heme, ferroprotoporphyrin IX; hemichrome, ferric bishistidyl hemoglobin; hemin, porphyrin group containing ferric iron; holo, heme (Fe^{2+})- or hemin (Fe^{3+})-containing; met, methemoglobin (ferric hemoglobin); ROS, reactive oxygen species; Mb, myoglobin; 5-FU, 5-fluorouracil; AHSP, α-hemoglobin stabilizing protein.

units with higher affinity and displace α from AHSP complexes in solution and *in vivo* (9, 10, 14, 24, 25). These observations indicate that AHSP can act as a molecular chaperone to bind nascent α-globin and stabilize its folding prior to incorporation into HbA during normal erythropoiesis (12, 14, 24, 25).

AHSP promotes dramatic biochemical changes to bound αO_2 (for review, see Ref. 26). Normally, α-globin heme iron is axially coordinated by His^{87}(F8), termed the proximal histidine. The opposite axial position binds dioxygen (O_2), which is stabilized by interaction with the distal histidine, His^{58}(E7) (27). AHSP binding to αO_2 accelerates spontaneous heme iron oxidation (autooxidation) from an Fe^{2+} (ferrous) to an Fe^{3+} (or met) state. Autooxidation is followed immediately by internal coordination of His^{58}(E7) to the hemin iron, resulting in a hexacoordinate bishistidyl or hemichrome structure (18, 21, 22, 28). Bishistidyl hemoglobins occur as α-globin degradation products in β-thalassemia (4, 6, 29, 30), during normal degradation of hemoglobin, and in some naturally occurring globins in mammalian tissues, plants, certain bacteria, and cold water fish (31–40). Binding of His^{58} to hemin iron appears to inhibit the ability of met-α to catalyze ROS production (39, 41). Thus, AHSP-mediated conversion of αO_2 to a bishistidyl state has been postulated to protect erythroid cells against oxidative damage during β-globin deficiency and/or oxidative stress. Although this possibility is supported by *in vitro* studies (22, 28), the *in vivo* relevance of AHSP-mediated conversion of bound αO_2 to the bishistidyl met-α state had not been examined until this study.

An evolutionarily conserved proline residue within loop 1 of AHSP regulates binding to ferrous αO_2 and its subsequent autooxidation (18). In the structure of the ASHP·met-α complex, the cis conformation at the AHSP Asp^{29}-Pro^{30} peptide bond projects loop 1 toward α-globin helix G where AHSP Pro^{30} promotes backbone hydrogen bonding interactions. Pro^{30} amino acid substitutions in AHSP convert the 29-30 peptide bond to a completely trans conformation, which generally enhances the affinity of AHSP for ferrous αCO and αO_2 and reduces the rates of autooxidation and subsequent conversion to the bishistidyl form (18).

Because of these large effects on AHSP affinity for reduced α subunits and on the redox and coordination properties of bound α subunits, we chose to examine the *in vivo* phenotypes of P30A and P30W variants of murine AHSP (18). Although these mutations significantly altered AHSP/αO_2 interactions *in vitro*, they surprisingly produced no detectable consequences in mice. These observations led us to re-examine α subunit binding, autooxidation, and hemin loss from the mutant AHSP complexes *in vitro*. Our combined *in vitro* and *in vivo* findings refine and revise current models for AHSP function during erythropoiesis and emphasize the physiological importance of high affinity met-α binding to AHSP.

EXPERIMENTAL PROCEDURES

Rates of α Subunit Binding and Release from Pro^{30} Variants—Detailed descriptions of measurements of α subunit binding to and release from AHSP variants are given in the accompanying paper by Mollan *et al.* (42). Time courses for association of reduced and oxidized α subunits with AHSP were measured in an Applied Photophysics PiStar kinetic stopped-flow spectrophotometer (Leatherhead, Surrey, UK), monitoring the intrinsic fluorescence of AHSP. The binding of holo-α subunits quenches the fluorescence of AHSP, and its release to β subunits restores the fluorescence emission. A detailed discussion of these signal changes and analysis of the observed time courses are also given in Mollan *et al.* (42).

Autooxidation Rates of AHSP·αO_2 Complexes—Autooxidation reactions were initiated by diluting a cold concentrated solution of αO_2 into an equimolar solution of AHSP in 0.1 M sodium phosphate, pH 7.0 at 37 °C and then recording optical absorbance visible spectra. Spectra were recorded using a Cary50Bio instrument (Varian, Inc., Palo Alto, CA). First-order rate constants for autooxidation to the hemichrome met-α were obtained by fitting the absorbance change time courses to a single exponential expression using the Microsoft Excel Solver plug-in (Microsoft Corp., Redmond, WA).

Rate of Hemin Loss from Oxidized α Subunits—Hemin dissociation time courses were measured by mixing the ferric form of α or α·AHSP with the apoglobin form of H64Y/V68F sperm whale myoglobin (Mb) as described previously for assaying hemin dissociation from metHb and metMb (43–46). Hemin loss from free ferric α generates α-apoglobin, which immediately precipitates at 37 °C, causing a dramatic increase in solution turbidity. Increasing solution turbidity interferes with monitoring the absorbance time courses at 600 nm for hemin transfer from α-globin to the apoMb reagent. To obtain analyzable time courses, the temperature was lowered to 10 °C, and 0.6 M sucrose was added to stabilize the apoprotein and inhibit precipitation (46). In addition, the reaction pH was lowered to 5.5 to speed up the reaction at the low temperature, which also helps prevent interference from apo-α-globin precipitation, particularly for free met-α subunits.

Hargrove *et al.* (44–46) have shown that hemin loss rates increase markedly at low pH as the proximal histidine becomes protonated. However, the relative effects of mutagenesis and oligomer dissociation for both Hbs and Mbs remain the same as that at higher, more physiological pH values. For the free met-αHb and met-α·AHSP complexes, the hemin loss reaction mixtures contained 6 μM met-α, 40 μM H64Y/V68F apoMb, 30 μM potassium ferricyanide to ensure oxidation, and 6 μM either WT, P30A, or P30W AHSP. Spectra were recorded every minute for ~12 h, and the increase at 600 nm is due to formation of the "green" H64Y/V68F holo-metMb complex as the α subunits lose hemin. Data were plotted as the normalized absorbance change at 600 nm *versus* time.

Animals—*Ahsp* P30W- and P30A-targeting constructs were generated by modification of a previously described *Ahsp*-targeting construct (supplemental Fig. 1) (10). Site-directed mutagenesis was used to replace the CCT codon for proline (Pro) with either GCT for alanine (P30A) or TGG for tryptophan (P30W). The targeting plasmids were linearized with SacI and electroporated into 129SV embryonic stem cells. Clones with stable integration of the targeting vector were selected with G418 and ganciclovir and further screened for homologous recombinants by Southern blotting and karyotyping. Selected clones were injected into C57BL/6 blastocysts to produce chimeric mice. These were bred with C57BL/6 mice (The

Jackson Laboratory, Bar Harbor, ME) to produce *Ahsp*$^{P30A/+}$ or *Ahsp*$^{P30W/+}$ heterozygotes. Neomycin selection cassettes were removed by interbreeding with E2A-Cre mice (47). Mice were genotyped using the primer set AHSP-KI-F (5′-AGA AAC GGG GGA TGC AAA TCC AAA ACA AAG-3′) and AHSP-KI-R (5′-CAA GTT CAC CCA GTC ATG AAC CAC AAT CAC-3′), generating a 190-base pair product for the wild-type allele and a 236-base pair product for the mutant allele. All mice used for experiments were backcrossed onto a C57BL/6 background for five to seven generations. *Ahsp*$^{-/-}$ mice were generated as described previously (10). β-Thalassemic (β-globin$^{Th3/+}$) mice were kindly provided by Oliver Smithies (University of North Carolina, Chapel Hill, NC) (48). The *Ahsp* allele is genetically linked to the β-globin (*Hbb*) locus (11); *Ahsp*/β-globin$^{Th3/+}$ double mutant mice were generated as described previously (11). Animal protocols were approved by the Institutional Animal Care and Use Committee of The Children's Hospital of Philadelphia (Philadelphia, PA).

Hematological Analysis—Mice were analyzed at 2 and 8 months of age. Blood was collected by submandibular bleeding, anticoagulated with EDTA, and analyzed on a Hemavet HV950FS analyzer (Drew Scientific, Dallas, TX). Reticulocyte counts were done using Retic-COUNT reagent according to the manufacturer's protocol using a FACSCalibur flow cytometer (BD Biosciences). Flow cytometry data were acquired using equipment maintained by the Flow Cytometry Core Laboratory of The Children's Hospital of Philadelphia Research Institute.

Intracellular ROS Detection—10^7 circulating erythrocytes were washed with Dulbecco's PBS (137 mM NaCl, 2.7 mM KCl, 8.1 mM Na_2HPO_4, 1.76 mM KH_2PO_4, pH 7.4 at 25 °C), loaded with 2′,7′-dichlorofluorescein diacetate (DCFH; Invitrogen) at 10 μM in PBS at 37 °C for 30 min, and washed again with PBS. Where indicated, H_2O_2 (Sigma-Aldrich) was added after DCFH loading at 10 or 100 μM in PBS, and cells were incubated at 37 °C for 30 min and washed again with PBS. DCFH mean fluorescence intensity was measured by flow cytometry using a FACSCalibur flow cytometer (BD Biosciences).

Detection of Globin Precipitates in Erythroid Cells—Analysis of globin precipitates in erythrocyte membrane skeletons was performed as described (11, 12, 49, 50). Briefly, 10 μl of washed red blood cells were lysed, and pellets were washed extensively in ice-cold 0.05× PBS (6.85 mM NaCl, 0.135 mM KCl, 0.41 mM Na_2HPO_4, 0.088 mM KH_2PO_4, pH 7.4 at 4 °C). Membrane lipids were extracted with 56 mM sodium borate, pH 8.0 at 4 °C. Precipitated globins were dissolved in 8 M urea, 10% acetic acid, 10% β-mercaptoethanol, and 0.04% pyronin; fractionated by Triton-acetic acid-urea gel electrophoresis; and stained with Coomassie Brilliant Blue. Soluble hemoglobin fractions were analyzed as loading controls. Gel electrophoresis was performed using a Mini-PROTEAN Tetra Cell apparatus (Bio-Rad).

AHSP Expression Analysis—Erythrocytes were lysed with 40 volumes of water with 1 mM dithiothreitol and 1:500 protease inhibitor mixture (Sigma-Aldrich). Bone marrow erythroid precursors were purified from mice of the indicated genotypes by immunomagnetic positive selection using the EasySep PE Selection Kit (StemCell Technologies, Vancouver, British Columbia, Canada) with Ter119-PE antibody (Biolegend, San Diego, CA) according to the manufacturer's instructions (51). Protein lysates from purified erythroblasts were prepared using radioimmune precipitation assay buffer with 1 mM DTT and 1:500 protease inhibitor mixture (Sigma-Aldrich). Protein concentrations were determined using a Pierce bicinchoninic acid assay kit (Thermo Scientific, Rockford, IL), and 10 μg of protein were resolved by 15% SDS-PAGE. After transfer to 0.2-μm PVDF membranes (Whatman), AHSP was detected using a rat polyclonal antibody raised against purified mouse AHSP protein and HRP-conjugated goat anti-rat secondary antibody. HRP-conjugated anti-β-actin antibody was used as a loading control. Western blots were developed using SuperSignal West Pico chemiluminescent reagent. Western blotting secondary antibodies, markers, and reagents were obtained from Thermo Scientific.

5-Fluorouracil (5-FU) Treatment to Induce Erythropoietic Stress—Mice were injected with 150 mg/kg 5-FU (Sigma-Aldrich) in normal saline intraperitoneally on day 0. On days 3, 9, 12, 15, 18, and 30, 15 μl of blood were collected from the tail vein into heparinized glass microhematocrit tubes (Globe Scientific, Paramus, NJ) for manual spin hematocrits and reticulocyte analysis.

Isoelectric Focusing of ^{35}S-Labeled Reticulocyte Extracts to Detect Globins and AHSP·αHb Complexes—10 μl of freshly collected erythrocytes and reticulocytes (normalized to reticulocyte percentage and hematocrit) were incubated in methionine/cysteine-free DMEM (Invitrogen), 2 mM L-glutamine, 10% dialyzed FBS, and 0.1 mM non-essential amino acids at 37 °C for 1 h. 50 μCi of ^{35}S-labeled methionine and cysteine (PerkinElmer Life Sciences) were added, and the cells were labeled for 10 min at 37 °C. The cells were washed with PBS and exposed to carbon monoxide to stabilize ferrous heme groups. The cells were lysed in 5 volumes of water, and the lysate was clarified by centrifugation. Lysates were resolved by isoelectric focusing (pH 6–8) on precast agarose gels from the Hemoglobin Test kit on an LKB 2117 Multiphor apparatus at 1500 V for 50 min (PerkinElmer Life Sciences). For autoradiography, gels were fixed in 10% trichloroacetic acid for 10 min, washed in deionized water, and dried. Images were acquired using a phosphor screen and Storm 865 scanner (GE Healthcare). Bands were quantified using National Institutes of Health ImageJ software. For analyzing band globin and AHSP content, isoelectric focusing gel bands were excised, boiled in 2× Laemmli sample buffer (4% SDS, 20% glycerol, 10% 2-mercaptoethanol, 0.004% bromphenol blue, 0.125 M Tris HCl, pH 6.8; Sigma-Aldrich), and proteins were resolved by 15% SDS-PAGE. Gels were either dried for autoradiography or used for mouse AHSP Western blotting as described above.

Statistical Methods—Statistical analysis was performed using GraphPad Prism 4.0 software (GraphPad Software, La Jolla, CA). All group comparisons were done using one-way analysis of variance.

Sequence Alignments—AHSP protein sequences were obtained using the Basic Local Alignment Search Tool (BLAST) at the NCBI using the human AHSP sequence (NCBI accession number NM_016633.2) as the query, and using the Ensembl genome browser. After manual inspection for sequence quality,

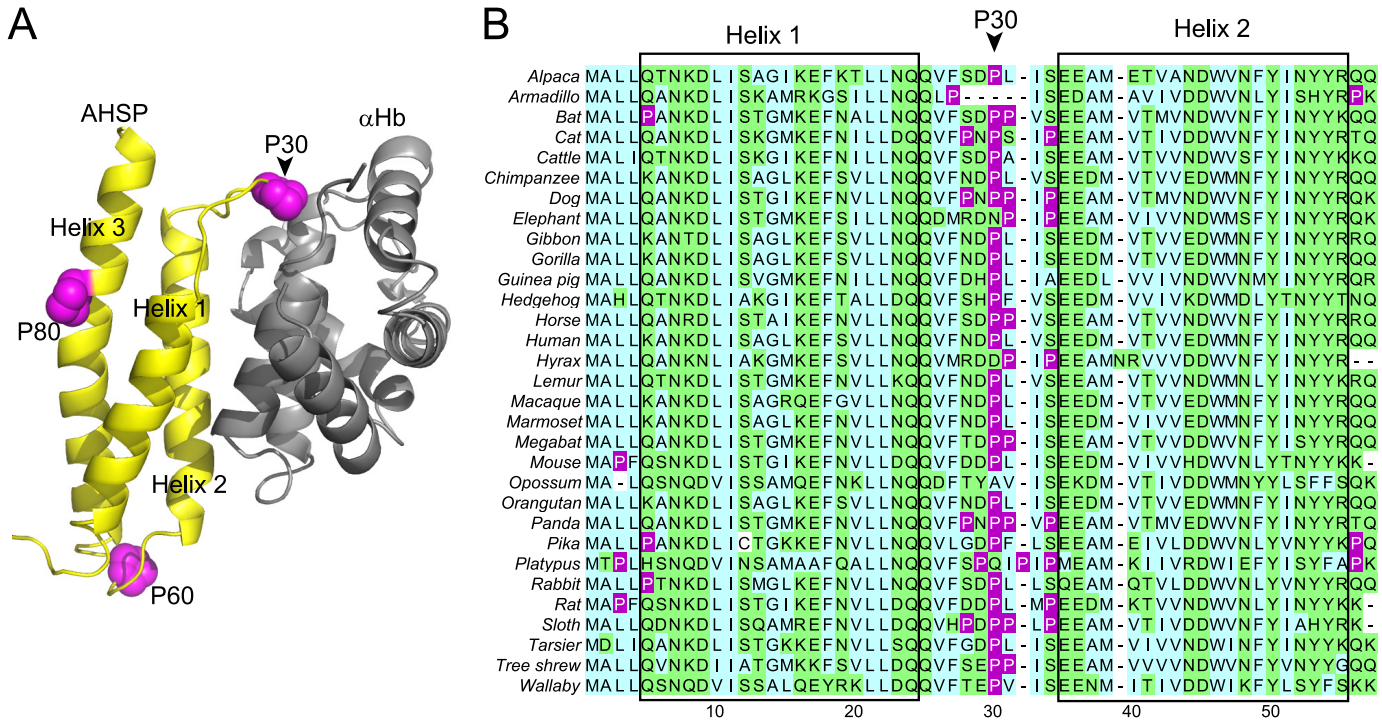

FIGURE 1. **Evolutionary and structural significance of AHSP proline 30.** *A*, structure of AHSP (*yellow*) bound to α-globin (*gray*) showing Pro^{30} at the interaction interface. Proline residues are shown in *purple*. The figure was generated using PyMOL software and Protein Data Bank code 1Z8U. *B*, ClustalW alignment comparing primary AHSP helix 1-loop 1-helix 2 amino acid sequences in different species, showing conservation of proline 30.

31 sequences were trimmed to include only helices 1 and 2 and aligned using the ClustalW algorithm with Strap multiple sequence alignment software (52).

RESULTS

AHSP Pro^{30} Mutations Alter α Chain Binding, Autooxidation, and Hemin Loss—The evolutionarily conserved proline at position 30 in loop 1 of AHSP contacts helix G of α-globin at the edge of the protein-binding interface (Fig. 1). To examine the function of this amino acid, Gell *et al.* (18) made a series of mutations that convert AHSP Pro^{30} to Gly, Ala, Val, Phe, and Trp and screened the resultant protein interactions with α-globin. Except for the P30G mutant, all AHSP variants showed enhanced affinity (lower K_D values) for ferrous αCO or αO_2 as measured by isothermal titration calorimetry. All of these mutants also showed 3–4-fold decreased rates of autooxidation and concomitant hemichrome formation (18).

In concert with our mutagenesis studies of the endogenous *Ahsp* gene, the *in vitro* effects of P30A and P30W AHSP substitutions were reevaluated for recombinantly produced proteins. Direct measurements of the association and dissociation rate constants for the binding of these AHSP variants to native αCO and met-α subunits were made using stopped-flow fluorescence methods as described in the accompanying paper by Mollan *et al.* (42) and as described previously (25). Direct comparisons of the speeds of $\alpha(Fe^{2+})CO$ and $met(Fe^{3+})\alpha$ binding to WT, P30A, and P30W AHSP are shown in Fig. 2*A*. Remarkably, the rates of binding of reduced and oxidized α subunits to AHSP were the same and were unaffected by mutation of Pro^{30} to either Ala or Trp. The only major difference is that WT AHSP showed a secondary slow phase when binding reduced α subunits. This slow phase for WT AHSP appears to be due to a cis to trans isomerization of Pro^{30} (see accompanying paper (42)).

In contrast, the rate of dissociation of α subunits from the AHSP complexes in the presence of excess β subunits depended markedly on both the oxidation state of the α-hemes and in the case of reduced αCO on the amino acid at position 30. As shown in Fig. 2*B*, reduced αCO was released from WT and P30A AHSP with half-times of roughly 2–4 s, whereas the half-time for dissociation from P30W AHSP was roughly 25-fold larger. In contrast, WT and both Pro^{30} AHSP mutants released oxidized α subunits very slowly with half-lives on the order of 200–400 s, similar to that for the release of reduced α subunits from the P30W mutant (Fig. 2*B*).

As a result of these differences in dissociation rate constants, the equilibrium dissociation constant (K_D) for α subunit binding depended strongly on the heme oxidation state. When the heme was reduced, the P30W AHSP mutant showed a ~30-fold higher affinity for α subunits than WT and P30A AHSP, which showed K_D values of roughly 20 nM. However, when the α subunits were oxidized, WT AHSP and the two Pro^{30} mutants showed the same high affinity with K_D values equal to 0.2–0.6 nM. Similar relative K_D differences for the AHSP variants were observed by isothermal titration calorimetry, although the isothermal titration calorimetry values were all 5–10-fold larger than those calculated from the association and dissociation rate constants. The cause of this discrepancy is discussed in Mollan *et al.* (42). The remarkably high affinity of AHSP for ferric α subunits and the lack of significant differences between the

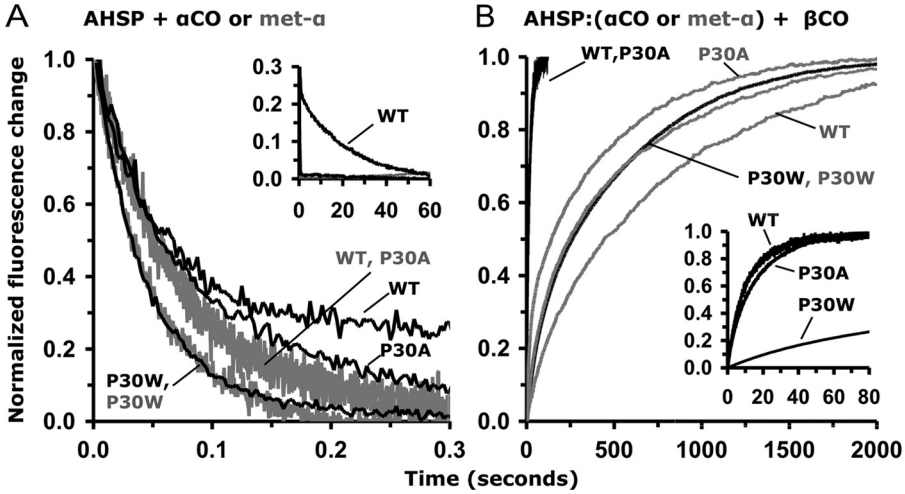

FIGURE 2. **Binding and release of reduced and oxidized α^{WT} to WT, P30A, and P30W AHSP.** *A*, time courses for 1 μM αCO (reduced, Fe^{2+}) or met-α (oxidized, Fe^{3+}) binding to 0.25 μM AHSP were measured in an Applied Photophysics PiStar stopped-flow spectrophotometer following decreases in intrinsic AHSP fluorescence. The binding of holo-α subunits quenches AHSP fluorescence due to resonance energy transfer to the heme. Observed fluorescence changes were normalized to allow direct comparisons among the AHSP variant and holo-α oxidation states, *i.e.* $(F_t - F_\infty)/(F_0 - F_\infty)$ where F_t, F_∞, and F_0 equal the fluorescence at time *t*, infinite time, and time 0, respectively. The *black lines* represent reactions with reduced αCO, and the *gray lines* represent reactions with oxidized met-α. *B*, time courses for the reaction of 8 μM βCO subunits with 0.25 μM AHSP·holo-α complexes. Under these conditions, the rate-limiting step is the dissociation of the α subunits from AHSP. As in *A*, the *black lines* represent dissociation of reduced αCO, and the *gray lines* represent dissociation of met-α. In these displacement reactions, the fluorescence of AHSP increases as α subunits dissociate from the complex, and the normalized increases were calculated as $1 - (F_t - F_\infty)/(F_0 - F_\infty)$. A detailed description of the reactions and analyses to obtain association (k'_{AHSP}) and dissociation (k_{AHSP}) rate constants is given in the accompanying paper (42). Finally, the fluorescence changes for the P30W AHSP mutant were roughly 2 times greater than those for either wild-type or P30A AHSP due to the "extra" Trp side chain.

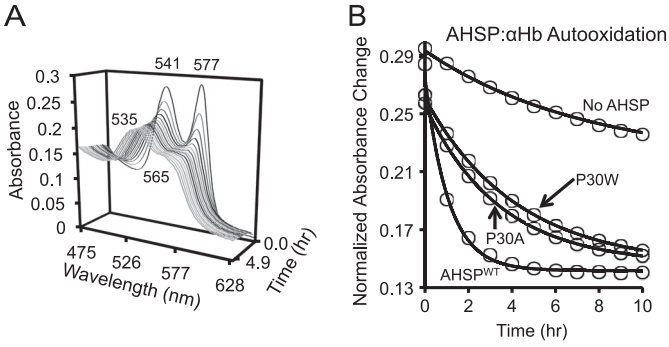

FIGURE 3. **Autooxidation of AHSP·αO_2 complexes.** *A*, absorbance spectra of 20 μM wild-type AHSP·αO_2 complexes over time during the autooxidation process. *B*, time courses for free αO_2 subunits and AHSP·α-globin complexes at 577 nm during the autooxidation process where the normalized absorbance changes were computed as $(A_t - A_\infty)/(A_0 - A_\infty)$ where A_t, A_∞, and A_0 equal the absorbance at time *t*, infinite time, and time 0, respectively. AHSP·αO_2 concentrations were fixed at 20 μM in 100 mM sodium phosphate buffer, pH 7.0 at 37 °C. Scans were taken every minute for ~24 h. Autooxidation of αO_2 subunits in the absence of AHSP was accompanied by an increase in solution turbidity due to precipitation at this temperature.

Pro^{30} mutants were discovered as a result of our efforts to understand the results of the *in vivo* mutagenesis studies.

Autooxidation of WT, P30A, and P30W AHSP·αO_2 complexes was also re-examined. As shown in Fig. 3, the rates of oxidation were 3–4-fold smaller than that for the wild-type complex as was observed by Gell *et al.* (18), but even these rates were still 2–3-fold greater than that for free αO_2 (Table 1). As estimated by increases in turbidity, the overall resistances of the AHSP·αO_2 complexes to precipitation were roughly the same for the wild type, P30A, and P30W AHSP (data not shown) even though the latter mutant·αO_2 complexes autooxidized more slowly. This observation and the lack of phenotype observed for mice expressing the mutant *Ahsp* genes (described in subsequent sections) led us to examine the rates of hemin loss from the oxidized hemichrome met-α·AHSP complexes.

Time courses for hemin loss were obtained by mixing AHSP·met-α complexes with excess H64Y/V68F apoMb as a hemin-scavenging reagent (Fig. 4). The ultrastable apoMb mutant turns "green" as indicated by the appearance of a large absorbance peak at 600 nm when it accepts hemin from a donor (44–46). Unexpectedly, the rates of hemin loss from the P30A and P30W AHSP·met-α complexes were 2–7-fold greater than that from the wild-type AHSP·met-α complex (Fig. 4 and Table 1). Unfortunately, the apo-α-globin product rapidly precipitates at 37 °C at pH 7, particularly in the absence of AHSP, and the resultant turbidity increases make quantitative analyses of hemin dissociation time courses impossible. However, the relative order of the initial rates of the absorbance increases at 600 nm for the wild-type and two variant AHSP·met-α complexes under these more physiological conditions was the same as the order of the rate constants determined quantitatively at low temperature and pH (not shown).

As shown in Fig. 4*B*, binding to wild-type AHSP enhanced the rate of hemin loss from met-α by a factor of 2. Binding to the Pro^{30} AHSP mutants accelerated hemin dissociation even further. These increases in k_{-hemin} seem to suggest increased exposure of the heme pocket to water in the AHSP complex. Liong *et al.* (53) have shown that exposing the proximal histidine to water causes dramatic (~1000-fold) increases in the rate of hemin loss from metMb variants. Thus, even partial unfolding of the heme pocket in the AHSP·met-α complexes to form the hemichrome would be expected to increase the rate of hemin loss markedly.

One key result in Table 1 is that the net resistance of the variant AHSP·αO_2 complexes to apoglobin formation, unfolding, and precipitation may be the same for all three variants.

TABLE 1

***In vitro* properties of AHSP P30A and P30W variants**

The bimolecular rate constants (k'_{AHSP}) for αCO binding to and the first-order dissociation rate constants for αCO release (k_{AHSP}) from wild-type AHSP and Pro^{30} mutants were measured at pH 7.0 at 25 °C in rapid mixing experiments (see Fig. 2 and Mollan *et al.* (42)). The equilibrium dissociation constants for αCO or met-α binding to AHSP under these conditions were calculated from k_{AHSP}/k'_{AHSP}. The first-order rates of autooxidation (k_{autox}) of αO_2 free in solution and bound to the AHSP variants were measured as described in Fig. 3. The first-order rates of hemin dissociation (k_{-hemin}) were measured as described in Fig. 4 at pH 5.5 at 10 °C to accelerate the process and prevent apoglobin precipitation before the hemin loss reaction was complete.

	αCO					
	k'_{AHSP}	k_{AHSP}	K_D	met-α K_D	k_{autox}, pH 7.0, 37 °C	k_{-hemin}, pH 5.5, 10 °C
	$\mu M^{-1}s^{-1}$	s^{-1}	$n M$	$n M$	h^{-1}	h^{-1}
AHSP WT	10.0	0.17	17 (93)[a]	0.17 (4.3)[1]	0.93	0.89
AHSP P30A	9.2	0.14	15 (38)[a]	0.60	0.29	1.9
AHSP P30W	13	0.0072	0.56 (7.7)[a]	0.24	0.24	6.2
No AHSP					0.13	0.50

[a] The numbers in parentheses indicate isothermal titration calorimetry data reported previously (18). These measurements are consistently higher than the values calculated from the rate constants. This discrepancy is discussed in the accompanying paper by Mollan *et al.* (42).

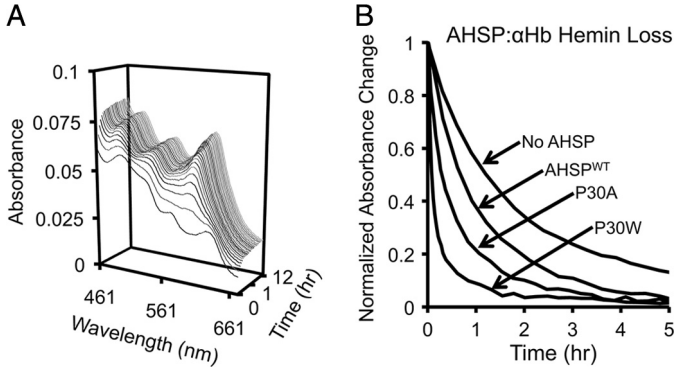

FIGURE 4. **Effects of AHSP mutations on rate of hemin loss from oxidized α subunits.** *A*, spectral changes for the reaction of 6 μM AHSP·met-α complexes with excess (40 μM) H64Y/V68F apoMb. The increase in absorbance at 600 nm indicates hemin gain by the H64Y/V68F Mb reagent. *B*, time courses for hemin dissociation from AHSP·met-α complexes plotted as the normalized absorbance change at 600 nm, *i.e.* $(A_t - A_\infty)/(A_0 - A_\infty)$ where A_t, A_∞, and A_0 equal the absorbance at time *t*, infinite time, and time 0, respectively. These experiments were conducted in 0.6 M sucrose, 200 mM sodium acetate buffer, pH 5.5 at 10 °C.

Even though the Pro^{30} mutant AHSP·αO_2 complexes autooxidized more slowly, the resultant AHSP·met-α complexes lost hemin more rapidly so that net rates of apo-α-globin appearance are probably similar for the Pro^{30} mutants and wild-type AHSP.

Generation of AHSP Pro^{30} Substitutions in Mice—We created *Ahsp*^{P30A} and *Ahsp*^{P30W} missense mutations in the endogenous murine gene (supplemental Fig. 1*A*). We reasoned that comparing hematologic parameters in these mutant strains would allow us to distinguish between effects caused by altered AHSP affinity for αO_2 and reduced rates of autooxidation and bishistidyl conversion. Mutant animals were born at normal Mendelian ratios, similar to what we observed previously for *Ahsp*$^{-/-}$ mice (10, 11). Erythroblast AHSP protein levels were normal in the mutant animals (supplemental Fig. 1*B*).

Analysis of AHSP·α-Globin Complexes in Vivo—Endogenous AHSP·α-globin complexes are more easily detected under conditions of α-globin excess (12, 48). Thus, we crossed the *Ahsp*^{P30W} and *Ahsp*^{P30A} mutant mice onto a β-thalassemia intermedia background (β-globin$^{Th3/+}$) (48) and examined the formation of mutant AHSP·α-globin complexes by isoelectric focusing of radiolabeled reticulocyte extracts (12). We detected several globin-containing bands that could potentially be an AHSP·α-globin complex (supplemental Fig. 2*A*). We used Western blotting of proteins isolated from these bands to identify the band that contained both α-globin and AHSP (supplemental Fig. 2*B*), allowing us to quantify the relative amount of labeled α-globin in the complex in subsequent experiments. Accumulation of the AHSP·α-globin complex was significantly increased in *Ahsp*$^{P30W/P30W}$ β-globin$^{Th3/+}$ mice consistent with biochemical studies showing that the mutant protein had increased affinity for α-globin (Fig. 5). AHSP·α-globin complexes were present at wild-type levels in *Ahsp*$^{P30A/P30A}$ β-globin$^{Th3/+}$ mice. Thus, it was possible to increase AHSP·α-globin complex formation *in vivo* through targeted mutagenesis of *Ahsp* gene as predicted from the higher affinity of P30W AHSP for reduced αO_2 or αCO *in vitro* (Fig. 5*B* and Table 1). However, our assay did not allow us to measure the fraction of the AHSP·α-globin complexes, which were in the bishistidyl hemichrome form *in vivo*.

Hematological Features of Ahsp^{P30A} and Ahsp^{P30W} Knock-in Mice—We first compared baseline erythropoiesis in AHSP Pro^{30}-substituted and control mice (Table 2A and supplemental Table 1). *Ahsp*$^{-/-}$ mice exhibited reticulocytosis and elevated red cell distribution width consistent with mild hemolysis. These parameters were entirely normal in *Ahsp*^{P30A} and *Ahsp*^{P30W} mutant mice (heterozygotes and homozygotes) at ages 2 (Table 2) and 8 months (not shown). *Ahsp*^{P30A} and *Ahsp*^{P30W} mouse erythrocytes exhibited normal morphology, whereas *Ahsp*$^{-/-}$ erythrocytes exhibited shape abnormalities and eosinophilic inclusions (Refs. 10 and 11 and data not shown). Of note, *Ahsp* mutant mice used in this study were backcrossed onto a C57BL/6 genetic background. In this pure strain, loss of *Ahsp* caused minimal anemia in contrast to *Ahsp*$^{-/-}$ mice with a mixed 129SV/C57BL/6 genetic background (10, 11).

Unstable α-globin resulting from β-thalassemia or loss of AHSP generates excessive ROS and membrane-bound Hb precipitates (Heinz bodies) (10, 11, 54–60). In AHSP Pro^{30}-substituted mice, membrane-bound insoluble globins were barely detectable in erythrocytes, similar to wild-type controls (Fig. 6*A*). Moreover, in contrast to *Ahsp*$^{-/-}$ mice, erythrocytes from *Ahsp*$^{P30W/P30W}$ and *Ahsp*$^{P30A/P30A}$ animals did not show increased ROS generation either at baseline (Fig. 6*B*) or after treatment with hydrogen peroxide (Fig. 6*C*). We also examined the abilities of *Ahsp* mutant mice to respond to increased erythropoietic demands after treatment with 5-FU, a nucleotide analog that destroys hematopoietic precursors, resulting in transient suppression of circulating blood cells (Fig. 7) (61, 62).

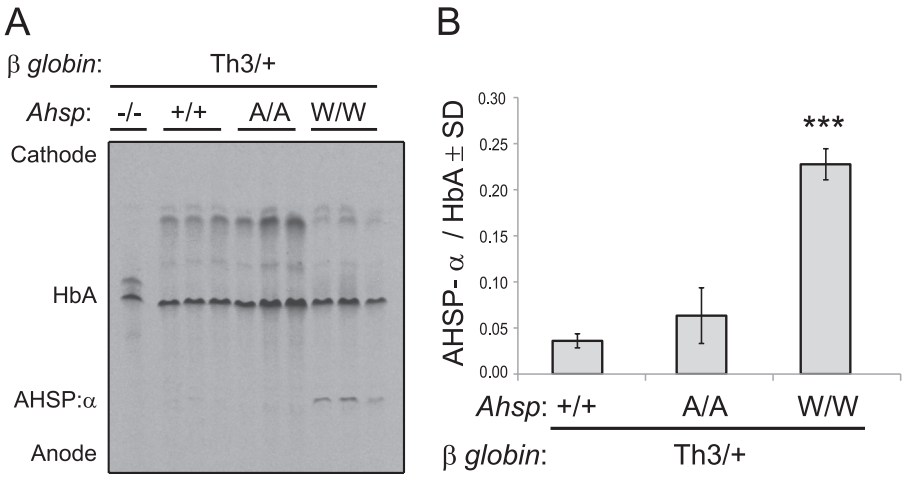

FIGURE 5. **AHSP P30W enhances AHSP/α-globin interaction *in vivo*.** *A*, the indicated AHSP·α-globin complexes were identified by isoelectric focusing according to control experiments outlined in supplemental Fig. 2. Reticulocytes from β-thalassemic (β-globin$^{Th3/+}$) mice with the indicated *Ahsp* genotypes (knock-out, wild type, and Pro^{30} amino acid substitutions) were labeled with [^{35}S]methionine/cysteine, lysed in the presence of carbon monoxide to stabilize globins, resolved by isoelectric focusing at pH 6–8, and detected by autoradiography. *B*, quantification of AHSP·α-globin complexes by autoradiography. Signals were normalized to the HbA signal. Three mice were analyzed from each group. *Error bars* show standard deviation. ***, $p < 0.001$ *versus* *Ahsp*$^{+/+}$.

TABLE 2

Key erythroid indices of AHSP Pro^{30} mutant mice at age 2 months in wild-type and β-thalassemia intermedia backgrounds

A, erythroid indices for mice with the indicated *Ahsp* genotypes. Data are shown as mean ± S.D. ***, $p < 0.001$; **, $p < 0.01$; *, $p < 0.05$ versus *Ahsp*$^{-/-}$ by one-way analysis of variance. No statistically significant differences were found between wild-type and Pro^{30} mutant *Ahsp* mice. B, erythroid indices of *Ahsp* Pro^{30} mutant/β-globin (*Hbb*) Th3/+ (β-thalassemia intermedia) mice. AHSP Pro^{30} missense mutations had no significant effects on erythroid indices of β-thalassemic mice. $p <$ 0.01 for all β-globin$^{+/+}$ *versus* β-globin$^{Th3/+}$ in all *Ahsp* genotypes by one-way analysis of variance. Additional hematological data from these experiments are summarized in supplemental Tables 1, 2, and 3.

A.	*Ahsp*^{P30A} mice			*Ahsp*^{P30W} mice			*Ahsp*$^{-/-}$
AHSP Genotype	**+/+**	**A/+**	**A/A**	**+/+**	**W/+**	**W/W**	**-/-**
Number of Mice	5	9	5	6	6	5	6
Hemoglobin (g/dL)	12.72 ± 0.55	12.61 ± 0.48	12.85 ± 1.28	13.20 ± 0.65	13.72 ± 0.63	12.40 ± 1.34	13.88 ± 0.69
Red Cell Distribution Width, RDW (%)	19.40 ± 1.04 ***	19.34 ± 2.30 ***	20.03 ± 0.46 **	18.98 ± 0.91 ***	18.87 ± 1.89 ***	18.00 ± 0.52 ***	**24.03 ± 1.00**
Reticulocytes (%)	2.04 ± 0.30 ***	2.87 ± 1.49 **	2.24 ± 0.67 **	3.08 ± 0.90*	2.84 ± 0.51**	2.84 ± 0.45*	**4.88 ± 1.77**

B. β *globin* (*Hbb*) genotype	**+/+**	**Th3/+ (β-thalassemia intermedia)**		
***Ahsp* Genotype**	**+/+**	**+/+**	**P30A/P30A**	**P30W/P30W**
Number of mice	18	22	11	7
Hemoglobin (g/dL)	13.15 ± 0.38	**9.32 ± 0.54**	**9.66 ± 0.55**	**9.54 ± 0.75**
Red Cell Distribution Width, RDW (%)	17.68 ± 0.74	**33.90 ± 2.56**	**35.97 ± 1.63**	**33.50 ± 3.27**
Reticulocytes (%)	2.48 ± 0.64	**22.81 ± 4.56**	**22.36 ± 1.97**	**20.67 ± 2.87**

Compared with control animals, the hematocrits of *Ahsp*$^{-/-}$ mice declined more rapidly after treatment with 5-FU, consistent with a reduced circulating lifespan of mutant erythrocytes (11). During subsequent recovery, there was increased reticulocytosis in the *Ahsp*$^{-/-}$ mice compared with controls. In contrast, *Ahsp*$^{P30W/P30W}$ and *Ahsp*$^{P30A/P30A}$ mice showed normal kinetics of erythrocyte decline and reticulocyte recovery after treatment with 5-FU. Together, these studies indicate that hemoglobin assembly and function are not impaired significantly by AHSP P30A or P30W substitution either at baseline or under conditions of erythropoietic stress despite substantial differences in α-globin binding affinity, induced rates of autooxidation, and hemin loss measured *in vitro*.

Effects of AHSP Pro^{30} Substitutions on β-Thalassemia Intermedia—Loss of AHSP exacerbates β-thalassemia intermedia (genotype β-globin$^{Th3/+}$) in mice (11). We postulated previously that in β-thalassemia AHSP may reduce the toxicity of excess free α-globin by converting it to a bishistidyl form, which exhibits a reduced rate of ROS generation (26). To test this model, we intercrossed β-globin$^{Th3/+}$ mice with animals harboring AHSP Pro^{30} substitutions. We reasoned that the AHSP P30A and AHSP P30W substitutions might have a greater impact on erythropoiesis in β-thalassemia, where α-globin is present in excess. The reduced rates of autooxidation of αO_2 and concomitant conversion to the hemichrome form when bound to the Pro^{30} AHSP mutants might aggravate β-thalassemia by increasing ROS generation in a manner similar to what was observed upon *Ahsp* gene ablation (11). Alternatively, the increased affinity of the AHSP mutants for ferrous α-globin (Table 1 and Fig. 5) might selectively enhance the ability of AHSP to protect against excess α-globin degradation and precipitation in β-thalassemia, particularly for the P30W mutant, which bound αO_2 about 30-fold more tightly.

AHSP proteins were expressed at similar levels in erythroid precursors of *Ahsp*$^{+/+}$, *Ahsp*$^{P30W/P30W}$, and *Ahsp*$^{P30A/P30A}$ mice with concomitant β-thalassemia (supplemental Fig. 3). Erythroid indices were indistinguishable between thalassemic mice expressing wild-type AHSP or either Pro^{30} mutation at 2 and 8 months (Table 2 and supplemental Tables 2 and 3). Moreover, the levels of erythroid membrane-associated α-globin precipitates were similar in β-thalassemic mice expressing wild-type AHSP and Pro^{30} mutations in contrast to those lacking AHSP where α-globin precipitation was increased (Fig. 8 and Ref. 11). Thus, the P30W and P30A substitutions have no detectable positive or negative effects on the ability of AHSP to protect against accumulation of toxic free α-globin in β-thalassemia.

DISCUSSION

Prior studies indicate two potential functions for AHSP during normal and pathologic erythropoiesis (8, 26, 63). First, AHSP acts as a molecular chaperone to bind and stabilize nascent α-globin folding intermediates prior to reaction with β-globin and assembly into HbA (Fig. 9). This function is gov-

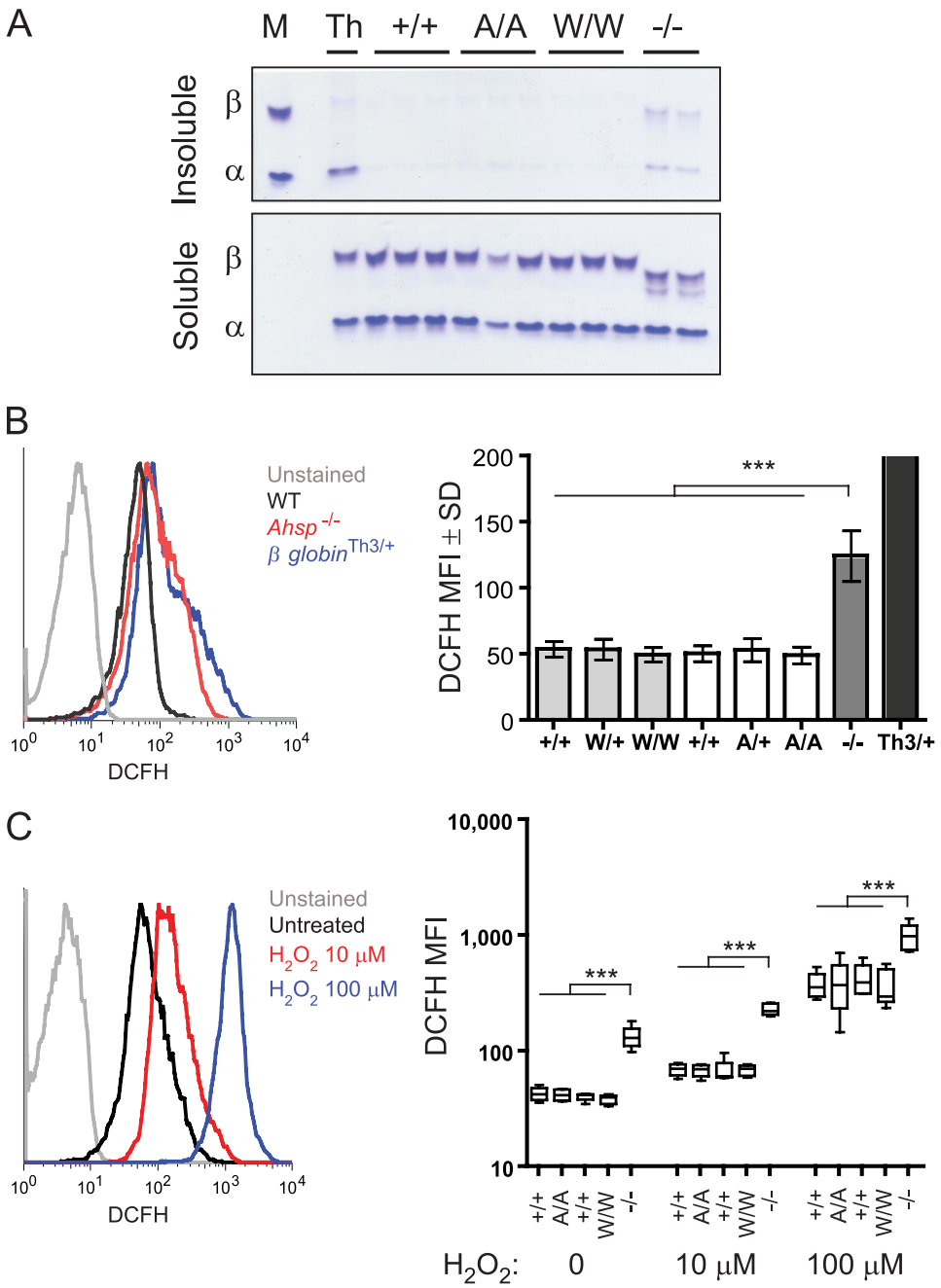

FIGURE 6. **AHSP Pro^{30} mutations do not destabilize α-globin or induce ROS production *in vivo*.** *A*, detection of membrane-bound insoluble globins. Equal numbers of circulating erythrocytes from mice with the indicated *Ahsp* genotypes were lysed, and insoluble fractions were analyzed for globin precipitates by Triton-acetic acid-urea gel electrophoresis. Migration positions of α- and β-globin are indicated in the marker (*M*) lane. Soluble fractions (1%) were included as loading controls. Erythrocytes from *Ahsp*$^{-/-}$ and β-thalassemic (β-globin$^{Th3/+}$) (*Th*) mice represent positive controls. *B*, circulating erythrocytes from mice with the indicated genotypes were stained with the ROS indicator DCFH and analyzed by flow cytometry. *Ahsp*$^{-/-}$ and β-thalassemic (β-globin$^{Th3/+}$) mice were analyzed as controls. Primary data are shown in the *left panel*. The *right panel* summarizes DCFH mean fluorescence intensities (*MFI*) for a group of mice ($n = 4–6$ for each genotype). ***, $p < 0.001$ *versus Ahsp*$^{-/-}$ genotype. *C*, circulating erythrocytes from mice with the indicated *Ahsp* genotypes were stained with DCFH, incubated with various concentrations of hydrogen peroxide (H_2O_2), and analyzed for ROS production by flow cytometry. Four to six mice were analyzed from each group. *Error bars* show standard deviation. ***, $p < 0.001$ *versus Ahsp*$^{-/-}$.

erned by the rates of holo- and apo-α-globin binding to and release from AHSP (18, 25, 42, 64). Thus, AHSP/α-globin interactions during HbA synthesis must be optimized to promote α-globin stability yet not interfere significantly with release of α-globin for binding to β-globin during HbA assembly.

Second, AHSP forms stable complexes with excess free α-globin under conditions of β-globin deficiency to reduce the toxicity associated with α-globin oxidation, hemin loss, and precipitation. Mitigation of excess α-globin toxicity was postulated to occur in part through AHSP-mediated conversion of bound α subunits to a bishistidyl, hemichrome state, which limits ROS production. Biochemical studies support this model, although it has been difficult to test *in vivo*. Pro^{30} regulates both the affinity of AHSP for reduced α-globin and the rate of conversion of bound αO_2 to the ferric bishistidyl met-α form (*i.e.* autooxidation).

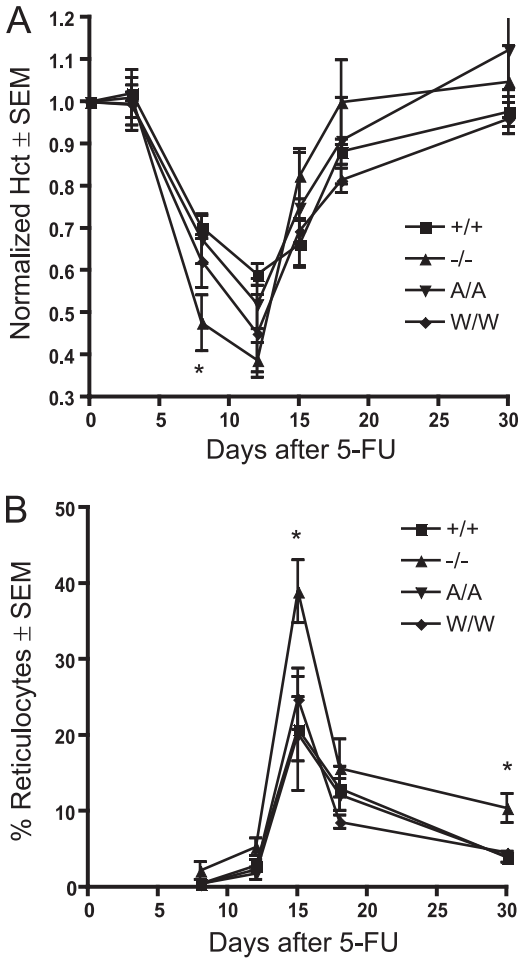

FIGURE 7. **AHSP Pro^{30} mutations do not affect stress erythropoiesis.** Normalized hematocrits (*Hct*) (*A*) and reticulocyte counts (*B*) of *Ahsp*$^{+/+}$, *Ahsp*$^{-/-}$, and *Ahsp* Pro^{30} mutant mice treated with 5-fluorouracil (150 mg/kg) and analyzed for 30 days are shown. Data are shown as mean ± S.E. Four to five mice of each genotype were analyzed. *, $p < 0.05$, one-way analysis of variance.

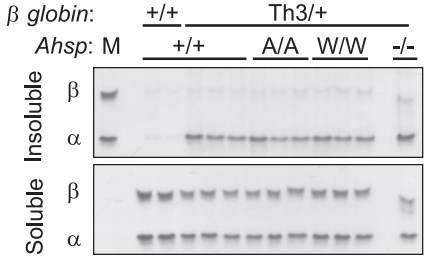

FIGURE 8. **AHSP proline 30 mutations do not alter globin precipitates in β-thalassemia.** Equal numbers of circulating erythrocytes from mice with the indicated *Ahsp* and β-globin genotypes were lysed, and insoluble fractions were analyzed for globin precipitates by Triton-acetic acid-urea gel electrophoresis. Migration positions of α- and β-globin are indicated in the marker (*M*) lane. Soluble fractions (1%) were included as loading controls.

To examine the importance of the latter properties *in vivo*, Pro^{30} missense mutations (P30A and P30W) were introduced into endogenous murine *Ahsp* loci. As shown in Table 1, these mutations significantly altered the biochemical properties of AHSP *in vitro*. However, in contrast to the complete loss of AHSP, the P30A and P30W substitutions produced no detectable *in vivo* effects on hemoglobin synthesis or stability at base line, during erythropoietic stress, or under conditions of α-globin excess (β-thalassemia) in mice.

This lack of phenotype for the *Ahsp* mutants requires the re-evaluation of current models for the physiological functions of AHSP during erythropoiesis and led us to re-examine the hypothesis that a major function of AHSP is to stabilize excess αO_2 by oxidizing it to a hemichrome species to prevent ROS generation. More generally, our work also highlights the importance of using *in vivo* approaches to test hypotheses generated by *in vitro* biochemical experiments, which in this case suggested that there should be marked physiological differences between the P30A and P30W variants and wild-type AHSP.

An alternative and perhaps complementary function of AHSP is to act as a molecular chaperone for α-globin during HbA assembly. This role is supported by kinetic studies showing that both ferrous and ferric holo-α bind ~20 times more rapidly to AHSP than to ferrous β subunits (14, 25, 42). However, β subunits have a 10,000-fold higher affinity for α-globin than AHSP due to an extremely small $\alpha 1\beta 1$ dissociation rate constant, which is on the order of 10^{-5} s^{-1} (25, 65). In comparison, the rate of α dissociation from AHSP is 10^2–10^4 larger for all the AHSP variants listed in Table 1. These kinetic results suggest that newly synthesized α-globin either with or without hemin binds initially to AHSP and subsequently is released for interaction with β-globin to form HbA (Fig. 9). At high AHSP and β-globin concentrations, the rate, but not the extent, of HbA assembly could be limited by the rate of release of α-globin from AHSP (Fig. 9) (25).

The AHSP concentration in late stage erythroblasts is ~0.1 mM (10). The concentration of HbA subunits is ~10–20 mM, although the concentrations of free, non-tetrameric α and β subunits are unknown (9, 10). One question is whether the ratio of AHSP to the pool of newly synthesized free β chains is sufficiently low for optimal speed of HbA assembly and how easily this process can be perturbed under physiological conditions. For example, increased AHSP concentration and/or enhanced affinity for α-globin could interfere with the rate of HbA tetramer formation. However, the ~30-fold increased affinity of AHSP P30W for αO_2 (Table 1) and the increased levels of the complex in reticulocytes (Fig. 5*B*) did not appear to impair the net amount of HbA synthesis in mouse erythrocytes. Moreover, 10-fold overexpression of AHSP does not reduce steady-state HbA concentrations in erythroid cells even during β-globin deficiency (66). Thus, experimental manipulation of both AHSP levels and its affinity for α subunit binding demonstrated that the ratio of AHSP to newly synthesized β-globin chains is not restrictive for HbA synthesis in mice.

All of these results suggest that within erythroblasts, the function of AHSP as a molecular chaperone for HbA assembly retains considerable plasticity to tolerate variations in α-globin interaction rates and affinities. The limitation appears to be the ratio of the rates of subunit denaturation *versus* formation of the initial stable oligomeric states, *i.e.* α·AHSP, β_4, and αβ complexes (Fig. 9). Once these homo- and heterocomplexes are formed, the subunits are stable enough to quantitatively reassemble into the holo-HbA tetramer, which is an effectively irreversible process.

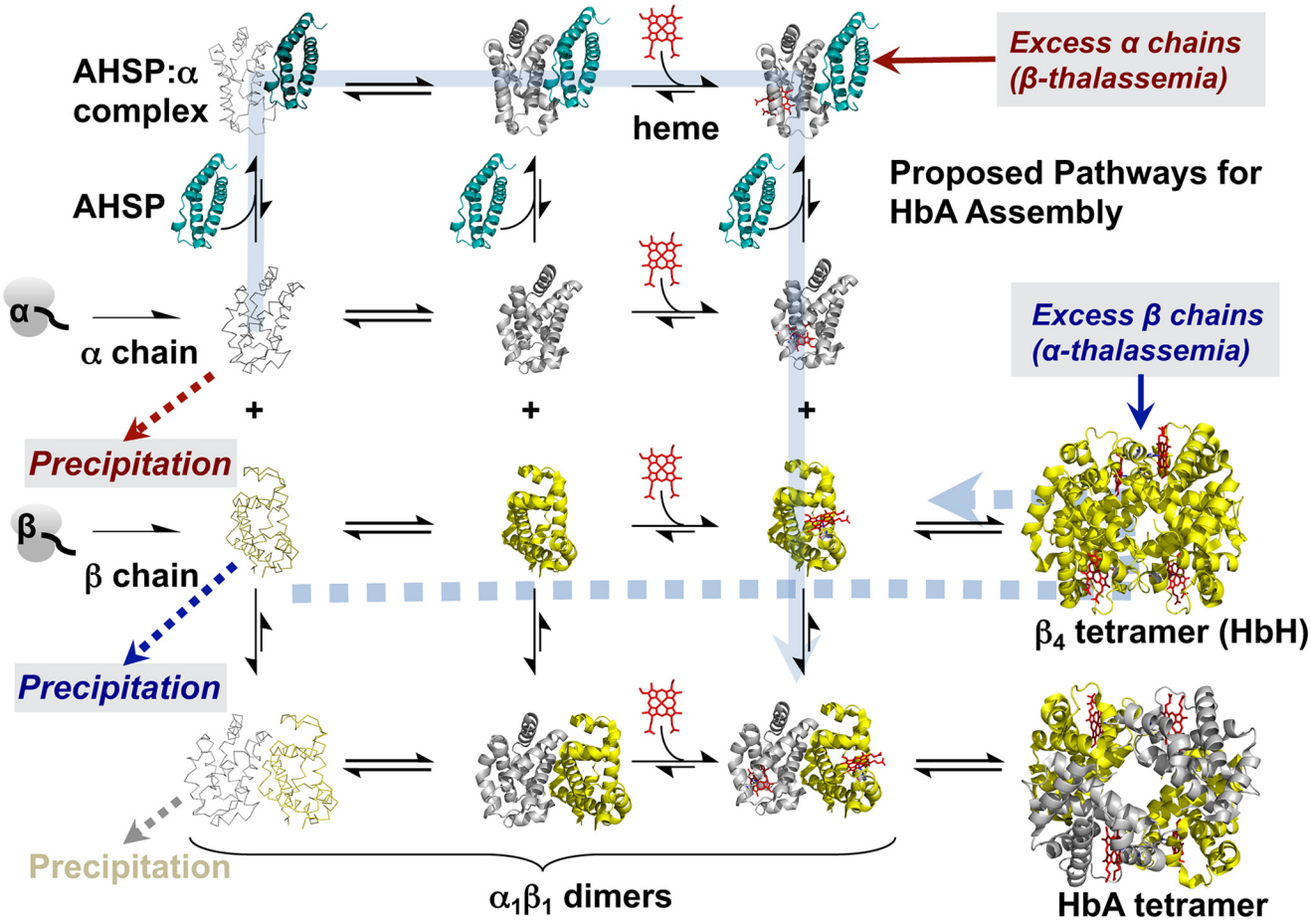

FIGURE 9. **Model for AHSP/α-globin interactions and hemoglobin assembly during erythropoiesis.** After translation, newly formed apo-α-globin subunits will precipitate rapidly unless they bind to their partner β subunit, AHSP, or free heme, which is in the ferric state (hemin). Both apo- and holo-β-globin subunits can self-assemble to form tetramers (*HbH*). Even in *Ahsp*$^{-/-}$ mice, almost normal concentrations of HbA are present in mature red cells, demonstrating that the simple assembly pathway indicated by the *lower* rung of reactions occurs readily. However, AHSP can facilitate assembly by stabilizing apo- and/or holo-α-globin folding intermediates and allow rapid displacement of AHSP by β-globin (*solid pale blue arrow*). There is a buildup of AHSP·α-globin complexes in β-thalassemia in addition to α-globin precipitates. In excess, β-globin can self-chaperone by forming β_4 tetramers (HbH), as is observed in α-thalassemia (*pale blue dashed arrow*).

The formation, spectral properties, and structure of AHSP·bishistidyl met-α complexes have been examined extensively *in vitro* (18, 21, 22, 28). The physiological function of this complex *in vivo* was examined in the current study by introducing endogenous *Ahsp* mutations that altered its rate of αO_2 autooxidation. AHSP amino acid substitutions that reduced this rate by 3–4-fold did not alter hemoglobin formation during normal erythropoiesis. Moreover, these mutations did not worsen β-thalassemia as might be expected if AHSP neutralizes the toxicity of free αO_2 by inducing formation of a stable and ROS-inhibiting bishistidyl structure. One explanation is that the lower autooxidation rates of the mutant AHSP·αO_2 complexes are still sufficient to generate a stable bishistidyl complex that prevents ROS formation and α-globin precipitation *in vivo*.

It seems more likely that the toxicity of excess αHb is due to hemin loss, apoglobin denaturation, and Heinz body formation, which is a major source of ROS in red cells. This explanation is supported by the lack of effect of the Pro^{30} mutations on erythropoiesis *in vivo*. Although the Pro^{30} mutant AHSP·αO_2 complexes autooxidized more slowly than the wild-type complex (Fig. 3 and Table 1), the mutant AHSP·met-α complexes lost hemin much more rapidly (Fig. 4). Thus, the resistance of the initial ferrous αO_2 complex to apo-α-globin formation is roughly the same for wild-type AHSP and the two variants, which could account for a lack of phenotype in the *Ahsp* mutant mice.

Finally, our findings and those presented in the accompanying paper (42) are also relevant to an unsolved problem concerning HbA synthesis. The redox state of heme during its insertion into apoglobins is not known. We suggest that during normal erythroid HbA assembly ferric heme is incorporated into AHSP-bound apo-α-globin, rapidly forming a hemichrome holo-α species with the heme pocket partially collapsed (Fig. 9). Subsequently, this intermediate is reduced by endogenous methemoglobin reductases to generate ferrous α-globin, which is released rapidly from AHSP for binding to β-globin.

Several lines of evidence support this model. Free ferrous heme (Fe^{2+}) autooxidizes rapidly in milliseconds to hemin (Fe^{3+}) even at low levels of O_2. Gell *et al.* (18) and others (64) have shown that AHSP binds and stabilizes apo-α-globin *in vitro*. Labeling studies in reticulocytes suggest that hemoglobin is initially synthesized with the heme in a ferric state (67,

68). As shown in Fig. 2*B* and Table 1, AHSP bound ferric met-α-globin with a 100-fold higher affinity than that for various reduced forms of α chains (18, 42). Culbertson and Olson (69) have shown that hemichrome species similar to that of the met-α·AHSP complex are key folding intermediates in the formation of holo-Hbs and holo-Mbs. Hemichrome α-globin bound to AHSP can be reduced anaerobically *in vitro* to generate fully folded, pentacoordinate deoxy-α with no evidence of a hemochrome species (bishistidyl coordination of ferrous iron) (28, 42, 69). *In vitro*, bishistidyl hemoglobins have faster reduction kinetics than pentacoordinate forms (70), suggesting that the α-globin hemichrome intermediate state induced by AHSP may facilitate reduction of the ferric heme iron *in vivo*.

Our new *in vitro* data also support this model of AHSP chaperone activity involving stabilization of an α ferric, hemichrome folding intermediate. The AHSP P30A and P30W mutations did not significantly affect the uptake and release of met-α-globin (see Fig. 2 and Table 1). Thus, although αO_2 autooxidation is impaired, the Pro^{30} mutations may have no detectable effects *in vivo* because the key function of AHSP is to prevent the precipitation of apo-α-globin conformers, facilitate uptake of hemin, stabilize the holo-met-α folding intermediate, and prevent release for binding to β-globin until the α-globin is reduced. These biochemical chaperone properties of AHSP have been exploited to enhance α-globin synthesis in bacterial expression systems (20) and to quantify the pool of free α chains in β-thalassemia (19). Although *in vitro* experiments have been valuable for establishing models of hemoglobin assembly and the role of AHSP, here we show that *in vivo* studies are required to test and refine these models. Further mutagenesis and *in vivo* studies will improve our understanding of AHSP/α-globin interactions and enhance the use of AHSP as a diagnostic and biotechnological tool.

Acknowledgments—We thank Dr. H. Franklin Bunn and Dr. Prem Ponka for helpful discussions.

REFERENCES

1. Perutz, M. F., Rossmann, M. G., Cullis, A. F., Muirhead, H., Will, G., and North, A. C. (1960) Structure of haemoglobin: a three-dimensional Fourier synthesis at 5.5-Å resolution, obtained by x-ray analysis. *Nature* **185,** 416–422
2. Dickerson, R. E., and Geis, I. (1983) *Hemoglobin: Structure, Function, Evolution, and Pathology*, Benjamin/Cummings Publishing Co., Menlo Park, CA
3. Steinberg, M. H. (2009) *Disorders of Hemoglobin: Genetics, Pathophysiology, and Clinical Management*, 2nd Ed., Cambridge University Press, Cambridge, UK
4. Rachmilewitz, E. A., Peisach, J., and Blumberg, W. E. (1971) Studies on the stability of oxyhemoglobin A and its constituent chains and their derivatives. *J. Biol. Chem.* **246,** 3356–3366
5. Antonini, E., Bucci, E., Fronticelli, C., Chiancone, E., Wyman, J., and Rossi-Fanelli, A. (1966) The properties and interactions of the isolated α- and β-chains of human haemoglobin. V. The reaction of α- and β-chains. *J. Mol. Biol.* **17,** 29–46
6. Rachmilewitz, E. A. (1974) Denaturation of the normal and abnormal hemoglobin molecule. *Semin. Hematol.* **11,** 441–462
7. Brunori, M., Falcioni, G., Fioretti, E., Giardina, B., and Rotilio, G. (1975) Formation of superoxide in the autoxidation of the isolated α and β chains of human hemoglobin and its involvement in hemichrome precipitation. *Eur. J. Biochem.* **53,** 99–104
8. Khandros, E., and Weiss, M. J. (2010) Protein quality control during erythropoiesis and hemoglobin synthesis. *Hematol. Oncol. Clin. North Am.* **24,** 1071–1088
9. Gell, D., Kong, Y., Eaton, S. A., Weiss, M. J., and Mackay, J. P. (2002) Biophysical characterization of the α-globin binding protein α-hemoglobin stabilizing protein. *J. Biol. Chem.* **277,** 40602–40609
10. Kihm, A. J., Kong, Y., Hong, W., Russell, J. E., Rouda, S., Adachi, K., Simon, M. C., Blobel, G. A., and Weiss, M. J. (2002) An abundant erythroid protein that stabilizes free α-haemoglobin. *Nature* **417,** 758–763
11. Kong, Y., Zhou, S., Kihm, A. J., Katein, A. M., Yu, X., Gell, D. A., Mackay, J. P., Adachi, K., Foster-Brown, L., Louden, C. S., Gow, A. J., and Weiss, M. J. (2004) Loss of α-hemoglobin-stabilizing protein impairs erythropoiesis and exacerbates β-thalassemia. *J. Clin. Investig.* **114,** 1457–1466
12. Yu, X., Kong, Y., Dore, L. C., Abdulmalik, O., Katein, A. M., Zhou, S., Choi, J. K., Gell, D., Mackay, J. P., Gow, A. J., and Weiss, M. J. (2007) An erythroid chaperone that facilitates folding of α-globin subunits for hemoglobin synthesis. *J. Clin. Investig.* **117,** 1856–1865
13. Yu, X., Mollan, T. L., Butler, A., Gow, A. J., Olson, J. S., and Weiss, M. J. (2009) Analysis of human α globin gene mutations that impair binding to the α hemoglobin stabilizing protein. *Blood* **113,** 5961–5969
14. Brillet, T., Baudin-Creuza, V., Vasseur, C., Domingues-Hamdi, E., Kiger, L., Wajcman, H., Pissard, S., and Marden, M. C. (2010) α-Hemoglobin stabilizing protein (AHSP), a kinetic scheme of the action of a human mutant, AHSPV56G. *J. Biol. Chem.* **285,** 17986–17992
15. Vasseur, C., Domingues-Hamdi, E., Brillet, T., Marden, M. C., and Baudin-Creuza, V. (2009) The α-hemoglobin stabilizing protein and expression of unstable α-Hb variants. *Clin. Biochem.* **42,** 1818–1823
16. Wajcman, H., Traeger-Synodinos, J., Papassotiriou, I., Giordano, P. C., Harteveld, C. L., Baudin-Creuza, V., and Old, J. (2008) Unstable and thalassemic α chain hemoglobin variants: a cause of Hb H disease and thalassemia intermedia. *Hemoglobin* **32,** 327–349
17. Turbpaiboon, C., Limjindaporn, T., Wongwiwat, W., U-Pratya, Y., Siritanaratkul, N., Yenchitsomanus, P. T., Jitrapakdee, S., and Wilairat, P. (2006) Impaired interaction of α-haemoglobin-stabilising protein with α-globin termination mutant in a yeast two-hybrid system. *Br. J. Haematol.* **132,** 370–373
18. Gell, D. A., Feng, L., Zhou, S., Jeffrey, P. D., Bendak, K., Gow, A., Weiss, M. J., Shi, Y., and Mackay, J. P. (2009) A *cis*-proline in α-hemoglobin stabilizing protein directs the structural reorganization of α-hemoglobin. *J. Biol. Chem.* **284,** 29462–29469
19. Vasseur, C., Pissard, S., Domingues-Hamdi, E., Marden, M. C., Galactéros, F., and Baudin-Creuza, V. (2011) Evaluation of the free α-hemoglobin pool in red blood cells: a new test providing a scale of β-thalassemia severity. *Am. J. Hematol.* **86,** 199–202
20. Vasseur-Godbillon, C., Hamdane, D., Marden, M. C., and Baudin-Creuza, V. (2006) High-yield expression in *Escherichia coli* of soluble human α-hemoglobin complexed with its molecular chaperone. *Protein Eng. Des. Sel.* **19,** 91–97
21. Feng, L., Gell, D. A., Zhou, S., Gu, L., Kong, Y., Li, J., Hu, M., Yan, N., Lee, C., Rich, A. M., Armstrong, R. S., Lay, P. A., Gow, A. J., Weiss, M. J., Mackay, J. P., and Shi, Y. (2004) Molecular mechanism of AHSP-mediated stabilization of α-hemoglobin. *Cell* **119,** 629–640
22. Feng, L., Zhou, S., Gu, L., Gell, D. A., Mackay, J. P., Weiss, M. J., Gow, A. J., and Shi, Y. (2005) Structure of oxidized α-haemoglobin bound to AHSP reveals a protective mechanism for haem. *Nature* **435,** 697–701
23. Santiveri, C. M., Pérez-Cañadillas, J. M., Vadivelu, M. K., Allen, M. D., Rutherford, T. J., Watkins, N. A., and Bycroft, M. (2004) NMR structure of the α-hemoglobin stabilizing protein: insights into conformational heterogeneity and binding. *J. Biol. Chem.* **279,** 34963–34970
24. Baudin-Creuza, V., Vasseur-Godbillon, C., Pato, C., Préhu, C., Wajcman, H., and Marden, M. C. (2004) Transfer of human α- to β-hemoglobin via its chaperone protein: evidence for a new state. *J. Biol. Chem.* **279,** 36530–36533
25. Mollan, T. L., Yu, X., Weiss, M. J., and Olson, J. S. (2010) The role of α-hemoglobin stabilizing protein in redox chemistry, denaturation, and hemoglobin assembly. *Antioxid. Redox Signal.* **12,** 219–231

26. Weiss, M. J., and dos Santos, C. O. (2009) Chaperoning erythropoiesis. *Blood* **113,** 2136–2144
27. Birukou, I., Schweers, R. L., and Olson, J. S. (2010) Distal histidine stabilizes bound O_2 and acts as a gate for ligand entry in both subunits of adult human hemoglobin. *J. Biol. Chem.* **285,** 8840–8854
28. Zhou, S., Olson, J. S., Fabian, M., Weiss, M. J., and Gow, A. J. (2006) Biochemical fates of α hemoglobin bound to α hemoglobin-stabilizing protein AHSP. *J. Biol. Chem.* **281,** 32611–32618
29. Mannu, F., Arese, P., Cappellini, M. D., Fiorelli, G., Cappadoro, M., Giribaldi, G., and Turrini, F. (1995) Role of hemichrome binding to erythrocyte membrane in the generation of band-3 alterations in β-thalassemia intermedia erythrocytes. *Blood* **86,** 2014–2020
30. Winterbourn, C. C., and Carrell, R. W. (1974) Studies of hemoglobin denaturation and Heinz body formation in the unstable hemoglobins. *J. Clin. Investig.* **54,** 678–689
31. Arredondo-Peter, R., Hargrove, M. S., Sarath, G., Moran, J. F., Lohrman, J., Olson, J. S., and Klucas, R. V. (1997) Rice hemoglobins. Gene cloning, analysis, and O_2-binding kinetics of a recombinant protein synthesized in *Escherichia coli*. *Plant Physiol.* **115,** 1259–1266
32. de Sanctis, D., Dewilde, S., Pesce, A., Moens, L., Ascenzi, P., Hankeln, T., Burmester, T., and Bolognesi, M. (2004) Crystal structure of cytoglobin: the fourth globin type discovered in man displays heme hexa-coordination. *J. Mol. Biol.* **336,** 917–927
33. Hankeln, T., Jaenicke, V., Kiger, L., Dewilde, S., Ungerechts, G., Schmidt, M., Urban, J., Marden, M. C., Moens, L., and Burmester, T. (2002) Characterization of *Drosophila* hemoglobin. Evidence for hemoglobin-mediated respiration in insects. *J. Biol. Chem.* **277,** 29012–29017
34. Perazzolli, M., Dominici, P., Romero-Puertas, M. C., Zago, E., Zeier, J., Sonoda, M., Lamb, C., and Delledonne, M. (2004) *Arabidopsis* nonsymbiotic hemoglobin AHb1 modulates nitric oxide bioactivity. *Plant Cell* **16,** 2785–2794
35. Pesce, A., Bolognesi, M., Bocedi, A., Ascenzi, P., Dewilde, S., Moens, L., Hankeln, T., and Burmester, T. (2002) Neuroglobin and cytoglobin. Fresh blood for the vertebrate globin family. *EMBO Rep.* **3,** 1146–1151
36. Pesce, A., Nardini, M., Dewilde, S., Ascenzi, P., Burmester, T., Hankeln, T., Moens, L., and Bolognesi, M. (2002) Human neuroglobin: crystals and preliminary x-ray diffraction analysis. *Acta Crystallogr. D Biol. Crystallogr.* **58,** 1848–1850
37. Sugimoto, H., Makino, M., Sawai, H., Kawada, N., Yoshizato, K., and Shiro, Y. (2004) Structural basis of human cytoglobin for ligand binding. *J. Mol. Biol.* **339,** 873–885
38. Vitagliano, L., Bonomi, G., Riccio, A., di Prisco, G., Smulevich, G., and Mazzarella, L. (2004) The oxidation process of Antarctic fish hemoglobins. *Eur. J. Biochem.* **271,** 1651–1659
39. Vergara, A., Vitagliano, L., Verde, C., di Prisco, G., and Mazzarella, L. (2008) Spectroscopic and crystallographic characterization of bis-histidyl adducts in tetrameric hemoglobins. *Methods Enzymol.* **436,** 425–444
40. Kakar, S., Hoffman, F. G., Storz, J. F., Fabian, M., and Hargrove, M. S. (2010) Structure and reactivity of hexacoordinate hemoglobins. *Biophys. Chem.* **152,** 1–14
41. Rifkind, J. M., Abugo, O., Levy, A., and Heim, J. (1994) Detection, formation, and relevance of hemichromes and hemochromes. *Methods Enzymol.* **231,** 449–480
42. Mollan, T. L., Khandros, E., Weiss, M. J., and Olson, J. S. (2012) Kinetics of α-globin binding to α-hemoglobin stabilizing protein (AHSP) indicate preferential stabilization of hemichrome folding intermediate. *J. Biol. Chem.* **287,** 11338–11350
43. Hargrove, M. S., Barrick, D., and Olson, J. S. (1996) The association rate constant for heme binding to globin is independent of protein structure. *Biochemistry* **35,** 11293–11299
44. Hargrove, M. S., Singleton, E. W., Quillin, M. L., Ortiz, L. A., Phillips, G. N., Jr., Olson, J. S., and Mathews, A. J. (1994) His^{64}(E7) → Tyr apomyoglobin as a reagent for measuring rates of hemin dissociation. *J. Biol. Chem.* **269,** 4207–4214
45. Hargrove, M. S., Wilkinson, A. J., and Olson, J. S. (1996) Structural factors governing hemin dissociation from metmyoglobin. *Biochemistry* **35,** 11300–11309
46. Hargrove, M. S., Whitaker, T., Olson, J. S., Vali, R. J., and Mathews, A. J. (1997) Quaternary structure regulates hemin dissociation from human hemoglobin. *J. Biol. Chem.* **272,** 17385–17389
47. Lakso, M., Pichel, J. G., Gorman, J. R., Sauer, B., Okamoto, Y., Lee, E., Alt, F. W., and Westphal, H. (1996) Efficient *in vivo* manipulation of mouse genomic sequences at the zygote stage. *Proc. Natl. Acad. Sci. U.S.A.* **93,** 5860–5865
48. Yang, B., Kirby, S., Lewis, J., Detloff, P. J., Maeda, N., and Smithies, O. (1995) A mouse model for β0-thalassemia. *Proc. Natl. Acad. Sci. U.S.A.* **92,** 11608–11612
49. Alter, B. P. (1981) Gel electrophoretic separation of globin chains. *Prog. Clin. Biol. Res.* **60,** 157–175
50. Sorensen, S., Rubin, E., Polster, H., Mohandas, N., and Schrier, S. (1990) The role of membrane skeletal-associated α-globin in the pathophysiology of β-thalassemia. *Blood* **75,** 1333–1336
51. Kina, T., Ikuta, K., Takayama, E., Wada, K., Majumdar, A. S., Weissman, I. L., and Katsura, Y. (2000) The monoclonal antibody TER-119 recognizes a molecule associated with glycophorin A and specifically marks the late stages of murine erythroid lineage. *Br. J. Haematol.* **109,** 280–287
52. Gille, C., and Frömmel, C. (2001) STRAP: editor for STRuctural Alignments of Proteins. *Bioinformatics* **17,** 377–378
53. Liong, E. C., Dou, Y., Scott, E. E., Olson, J. S., and Phillips, G. N., Jr. (2001) Waterproofing the heme pocket. Role of proximal amino acid side chains in preventing hemin loss from myoglobin. *J. Biol. Chem.* **276,** 9093–9100
54. Rouyer-Fessard, P., Garel, M. C., Domenget, C., Guetarni, D., Bachir, D., Colonna, P., and Beuzard, Y. (1989) A study of membrane protein defects and α hemoglobin chains of red blood cells in human β thalassemia. *J. Biol. Chem.* **264,** 19092–19098
55. Joshi, W., Leb, L., Piotrowski, J., Fortier, N., and Snyder, L. M. (1983) Increased sensitivity of isolated α subunits of normal human hemoglobin to oxidative damage and crosslinkage with spectrin. *J. Lab. Clin. Med.* **102,** 46–52
56. Advani, R., Sorenson, S., Shinar, E., Lande, W., Rachmilewitz, E., and Schrier, S. L. (1992) Characterization and comparison of the red blood cell membrane damage in severe human α- and β-thalassemia. *Blood* **79,** 1058–1063
57. Schrier, S. L., Rachmilewitz, E., and Mohandas, N. (1989) Cellular and membrane properties of α and β thalassemic erythrocytes are different: implication for differences in clinical manifestations. *Blood* **74,** 2194–2202
58. Scott, M. D., van den Berg, J. J., Repka, T., Rouyer-Fessard, P., Hebbel, R. P., Beuzard, Y., and Lubin, B. H. (1993) Effect of excess α-hemoglobin chains on cellular and membrane oxidation in model β-thalassemic erythrocytes. *J. Clin. Investig.* **91,** 1706–1712
59. Shinar, E., Rachmilewitz, E. A., and Lux, S. E. (1989) Differing erythrocyte membrane skeletal protein defects in α and β thalassemia. *J. Clin. Investig.* **83,** 404–410
60. Shinar, E., Shalev, O., Rachmilewitz, E. A., and Schrier, S. L. (1987) Erythrocyte membrane skeleton abnormalities in severe β-thalassemia. *Blood* **70,** 158–164
61. Li, B., Jia, N., Kapur, R., and Chun, K. T. (2006) Cul4A targets p27 for degradation and regulates proliferation, cell cycle exit, and differentiation during erythropoiesis. *Blood* **107,** 4291–4299
62. Bogacheva, O., Bogachev, O., Menon, M., Dev, A., Houde, E., Valoret, E. I., Prosser, H. M., Creasy, C. L., Pickering, S. J., Grau, E., Rance, K., Livi, G. P., Karur, V., Erickson-Miller, C. L., and Wojchowski, D. M. (2008) DYRK3 dual-specificity kinase attenuates erythropoiesis during anemia. *J. Biol. Chem.* **283,** 36665–36675
63. Favero, M. E., and Costa, F. F. (2011) α-Hemoglobin-stabilizing protein: an erythroid molecular chaperone. *Biochem. Res. Int.* **2011,** 373859
64. Krishna Kumar, K., Dickson, C. F., Weiss, M. J., Mackay, J. P., and Gell, D. A. (2010) AHSP (α-haemoglobin-stabilizing protein) stabilizes apo-α-haemoglobin in a partially folded state. *Biochem. J.* **432,** 275–282
65. Adachi, K., Zhao, Y., and Surrey, S. (2002) Assembly of human hemoglobin (Hb) β- and γ-globin chains expressed in a cell-free system with α-globin chains to form Hb A and Hb F. *J. Biol. Chem.* **277,** 13415–13420
66. Nasimuzzaman, M., Khandros, E., Wang, X., Kong, Y., Zhao, H., Weiss, D., Rivella, S., Weiss, M. J., and Persons, D. A. (2010) Analysis of α hemoglobin stabilizing protein overexpression in murine β-thalassemia. *Am. J. Hema-*

tol. **85,** 820–822
67. Schulman, H. M. (1974) Evidence that ferrihemoglobin may function as an intracellular heme carrier in reticulocytes. *Can. J. Biochem.* **52,** 665–669
68. Schulman, H. M., Martinez-Medellin, J., and Sidloi, R. (1974) The oxidation state of newly synthesized hemoglobin. *Biochem. Biophys. Res. Commun.* **56,** 220–226
69. Culbertson, D. S., and Olson, J. S. (2010) Role of heme in the unfolding and assembly of myoglobin. *Biochemistry* **49,** 6052–6063
70. Weiland, T. R., Kundu, S., Trent, J. T., 3rd, Hoy, J. A., and Hargrove, M. S. (2004) Bis-histidyl hexacoordination in hemoglobins facilitates heme reduction kinetics. *J. Am. Chem. Soc.* **126,** 11930–11935